Band Gap Engineering via Edge-Functionalization of Graphene Nanoribbons

Philipp Wagner, Christopher Ewels, Jean-Joseph Adjizian, Laurence Magaud, Pascal Pochet, Stephan Roche, Alejandro Lopez-Bezanilla, Viktoria V. Ivanovskaya, Abu Yaya, Mark Rayson, et al.

Band Gap Engineering via Edge-Functionalization of Graphene Nanoribbons

Philipp Wagner,[†] Christopher P. Ewels,*[,†] Jean-Joseph Adjizian,[†] Laurence Magaud,[‡] Pascal Pochet,[§] Stephan Roche,[∥,⊥] Alejandro Lopez-Bezanilla,[#] Viktoria V. Ivanovskaya,[▽] Abu Yaya,[○] Mark Rayson,[◆] Patrick Briddon,[†,¶] and Bernard Humbert[†]

[†]Institut des Matériaux Jean Rouxel (IMN), Université de Nantes, CNRS UMR 6502, F-44322 Nantes, France

[‡]Institut Néel, CNRS-UJF, BP 166, F-38042 Grenoble, France

[§]Laboratoire de simulation atomistique (L Sim), SP2M, INAC, CEA-UJF, F-38054 Grenoble, France

[∥]ICN2 - Institut Català de Nanociència i Nanotecnologia, Campus UAB, Bellaterra 08193, Barcelona, Spain

[⊥]ICREA - Institució Catalana de Recerca i Estudis Avancats 08010, Barcelona, Spain

[#]Argonne National Laboratory, 9700 South Cass Avenue, Argonne, Illinois 60439, United States

[▽]Unité Mixte de Physique CNRS-Thales, 91767 Palaiseau, and Université Paris-Sud F-91405, Orsay, France

[○]Department of Materials Science and Engineering, University of Ghana, P.O. Box 24, Legon, Accra, Ghana

[◆]Department of Chemistry, University of Surrey, Guildford, Surrey GU2 7XH, United Kingdom

[¶]School of Electrical, Electronic and Computer Engineering, University of Newcastle, Newcastle upon Tyne NE1 7RU, United Kingdom

ABSTRACT: Density functional calculations are used to perform a systematic study of the effect of edge-functionaliza-tion on the structure and electronic properties of graphene nanoribbons (GNRs). −H, −F, −Cl, −Br, −S, −SH, and−OH edge-functionalization of armchair, zigzag, and recon-structed Klein-type GNRs was considered. The most energeti-cally favorable edge structure varies depending on the choice of functional group. It is shown, for the first time, that reconstructed Klein-type GNRs are important stable configurations for several edge-functional groups. Band gaps using three different exchange-correlation functionals are calculated. The band gap for armchair GNRs can be tuned over a range of 1.2 eV by varying the edge-functional groups. In contrast, the band gaps of zigzag and reconstructed Klein edge GNRs are largely insensitive to the choice of edge-functional group, and ribbon width is instead the defining factor. Alternatively, the armchair GNR band gap can be controlled by varying the number of functional groups per opposing edge, altering the GNR "effective" width. Edge-functionalization design is an appropriate mechanism to tune the band gap of armchair GNRs.

INTRODUCTION

While graphene exhibits great promise for use in electronic devices,[1−3] one of the major limitations of an ideal infinite graphene sheet is its lack of an electronic band gap.[4] One solution to this problem is to work with thin strips of graphene, so-called graphene nanoribbons (GNRs),[5] which demonstrate finite band gaps.[6−8] The characteristics of thin, straight GNRs are dominated by the precise nature of their edges.[5,9−13] Edge engineering has been proposed as a route to tailor various properties of graphene[14−18] and hexagonal boron nitride nanoribbons.[19−21]

For (unreconstructed) graphene edges, armchair or zigzag edges are both possible,[22−24] giving armchair GNRs (AGNRs) and zigzag GNRs (ZGNRs) with well-defined widths.[5,6,25] A mix of these different edge types results in chiral edges[5,26] and chiral graphene nanoribbons (CGNRs). All of these graphene edge types have been identified in atomic resolution transmission electron microscopy (HRTEM).[27−29] An alternative graphene edge configuration was also proposed and experimentally confirmed, the Klein edge.[29,30] Further, it has been recently shown theoretically that pairwise reconstruction of Klein edges adds stability,[31] especially when hydrogenated.[32] Additionally, such graphene edges lead to reconstructed Klein GNRs (RKGNRs).[32]

In 2010, atomically precise AGNRs (with width 7, defined as the number of rows of carbon atoms parallel to the ribbon axis, referred to as 7-AGNR hereafter) were successfully assembled via a bottom-up process by Cai and co-workers.[33] The ability to grow a single specific ribbon width is an important prerequisite for designing and hence tuning GNR electronic properties for future carbon-based electronic devices.[16,18,34−36] First studies exploring hydroxyl (−OH) functionalized edges (among others) of thin AGNRs have shown the significant influence of chemical addends to structural, electronic, mechanical, and

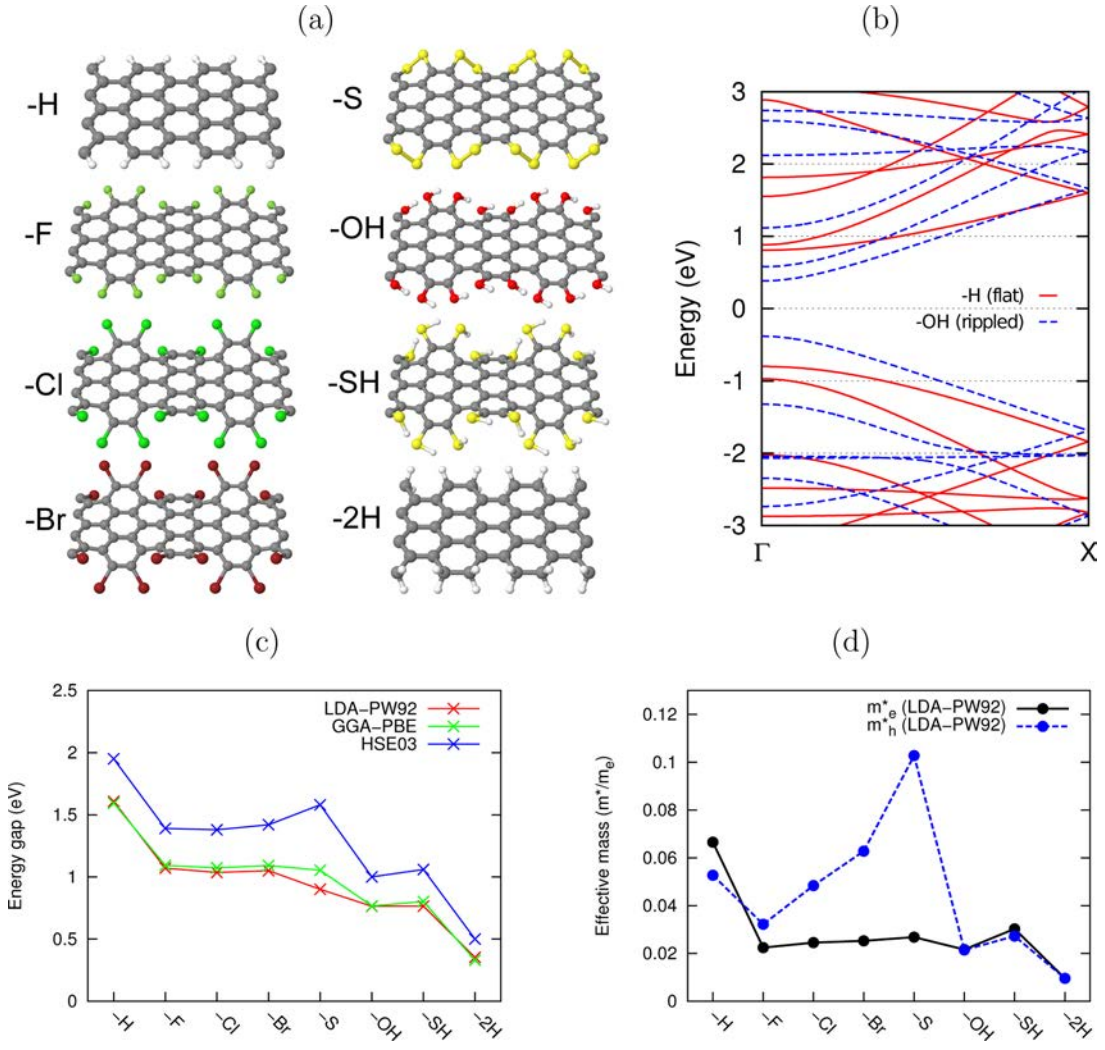

Figure 1. (a) Structures of different functionalized width 7 AGNRs. (b) LDA-PW92 band structures showing band dispersion along the ribbon axis for −H and −OH termination. (c) Calculated band gaps using different exchange-correlation implementations (LDA-PW92, GGA-PBE, and HSE03) (see Table 1). (d) LDA-PW92 effective electron (m_e^*) and hole (m_h^*) masses at the Γ-point of the AGNRs.

vibrational properties.[18,37] More recently, oxygen (−O), nitrogen (−N), fluorine (−F), chlorine (−Cl), and again hydroxyl (−OH)-functionalized AGNRs were studied.[38,39] Nevertheless, the literature is missing a complete study covering the full range of graphene edge types with different functional addends, at consistent levels of theory. Such a reference, how to tailor ribbon composition toward specific electronic behavior, would serve as an important guide for experimental synthesis groups in the future.

For this reason, in this Article a detailed theoretical investigation of the influence of edge-functionalization is presented, using hydrogen (−H), fluorine (−F), chlorine (−Cl), bromine (−Br), sulfur (−S) atoms, and −SH and −OH groups, on a width 7 armchair GNR, a width 6 zigzag GNR, and for the first time on a width 6 reconstructed Klein GNRn.[32] An overview is given of the influence of these edge-functional groups attached to these different graphene nanoribbon types, focusing on structural and electronic ribbon properties (especially the band gap). Additionally, the dependence of armchair GNR band gap value on functionalization and theoretical method is explored, to better classify such calculated results. Finally, an alternative route to tune AGNR electronic properties, by introducing an effective reduction of the ribbon width through different hydrogenation of its two opposing edges, is reviewed.

METHOD

Density functional theory (DFT) calculations using LDA-PW92[40] and GGA-PBE functionals[41] were performed as implemented in the AIMPRO code.[42−44] The calculations were carried out using supercells, fitting the charge density to plane waves with an energy cutoff of 150 Ha (Ha: Hartree energy). Electronic level occupation was obtained using a Fermi occupation function with kT = 0.04 eV. Relativistic pseudopotentials are generated using the Hartwingster−Goedecker−Hutter scheme.[45] Periodic boundary conditions have been applied by using supercells. Supercell sizes have been checked and chosen to be sufficiently large (vacuum distance between ribbons larger than 12 Å) to avoid interaction with neighboring ribbons. All calculations were performed using orthorhombic supercells. A fine k-point grid was chosen (armchair GNR, $(12/N) \times 1 \times 1$ and zigzag/reconstructed Klein GNR, $(18/N) \times 1 \times 1$, where N is the number of fundamental graphene unit cells along the ribbon axis). Energies have converged to better than 10^{-7} Ha. Atomic positions and lattice parameters were geometrically optimized

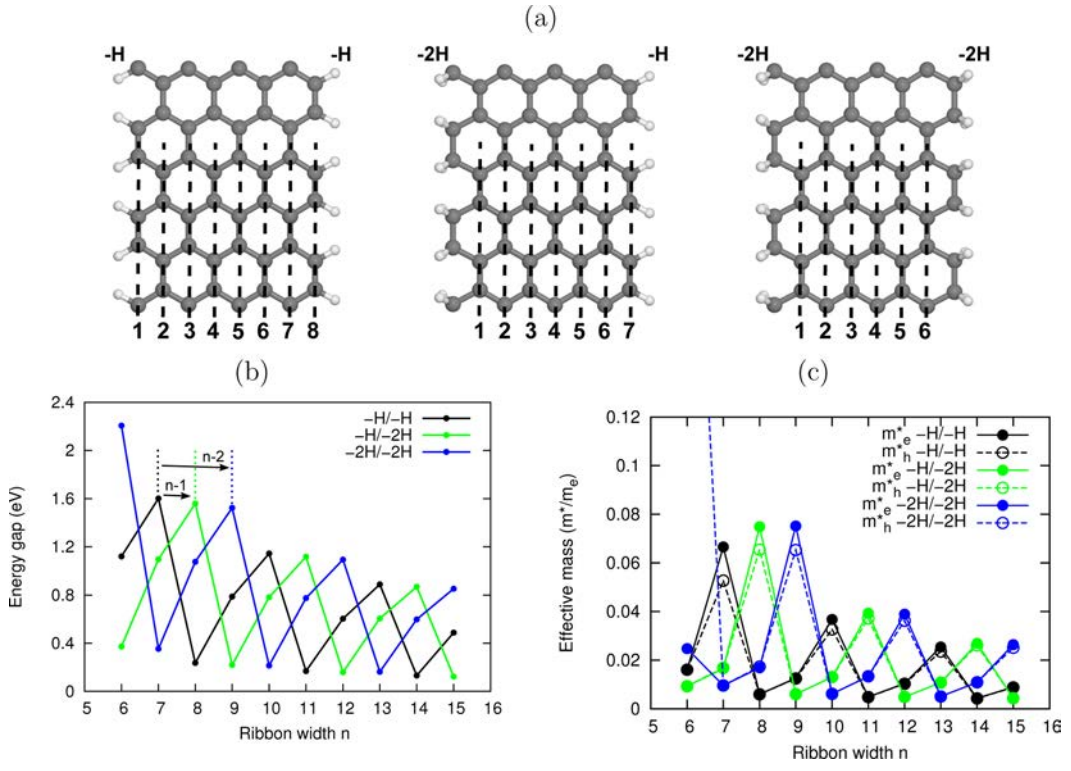

Figure 2. (a) The three different hydrogenated edge symmetries "−H/−H", "−2H/−H", and "−2H/−2H". Below each structure, the effective width derived from the sp^2 network is given. (b) LDA-PW92 band gaps with characteristic 3*N* periodicity calculated for different H-terminations of opposed armchair edges. (c) LDA-PW92 effective electron (m_e^*) and hole (m_h^*) masses at the Γ-point of the AGNRs. The width in both graphs is given in respect of the simple carbon atom ribbon width, the "−H/−H" case.

until the maximum atomic position change in a given iteration dropped below 10^{-5} a_0 (a_0: Bohr radius).

HSE03 band gap calculations for the width 7 AGNRs have been performed with the code VASP[46] and the HSE03 functional[47] with the same supercells and *k*-point meshes as described before, using the LDA-PW92 geometrically optimized atomic positions.

Width 7 armchair nanoribbons (7-AGNRs) have seven rows of carbon atoms parallel to the ribbon axis. Width 6 zigzag ribbons (6-ZGNRs) have six zigzag rows of carbon atoms (carbon chains) parallel to the ribbon axis. Width 6 reconstructed Klein ribbons (6-RKGNRs) also have six zigzag rows of unfunctionalized carbon atoms parallel to the ribbon axis; that is, sp^3-C atoms at the edge are not included in the width definition. Ribbon width is discussed further in the relevant sections below.

RESULTS

Armchair Graphene Nanoribbons (AGNRs). While hydrogenated graphene edges are flat, the steric hindrance between larger functional groups −F, −Br, −Cl, −S, −OH, and −SH has been shown to cause armchair edges to form static out-of-plane distorted ripples.[18,37,38] More recently, similar edge rippling has been predicted for −OH edge-functionalized BN armchair nanoribbons.[21] In the present study, out-of-plane edge rippling has been taken into account for all types of functional groups attached to AGNRs, shown in Figure 1a. Here, we use free-standing AGNRs with opposing edges terminated identically. Further, for the width 7 AGNR, the influence of the edge-functional groups −H, −2H, −F, −Br, −Cl, −S, −OH, and −SH on ribbon band gap was calculated using different treatments for the exchange-correlation energy (LDA-PW92, GGA-PBE, and HSE03), as shown in Figure 1c. The well-known band gap underestimation in LDA and PBE-GGA calculations is confirmed.[48,49] While qualitatively all band gaps show similar trends, an average deviation of 20−30% was found using LDA-PW92 and GGA-PBE as compared to calculations using a HSE03 functional, in good agreement with prior literature.[7] Using GW calculations, the gap of a singly hydrogenated width 7 AGNR is found even larger at about ∼3.7 eV.[8,50,51] Experimentally, the band gap of a simple hydrogenated width 7 AGNR on an Au(111) surface was measured to be ∼2.3 eV.[51]

These results show it is possible to tune the ribbon band gap over a wide energy range of 1.2 eV through correct choice of ribbon edge-functionalization. Notably, halogenation results in reduction in band gap of over 0.5 eV as compared to equivalent hydrogenated ribbons. We note that larger band gaps are normally concomitant with lower mobilities at the band edges (larger effective carrier masses, see Figure 1d), showing that transport properties can be dramatically modified depending on the nature of edge-functionalization.[52,53] This variation in band curvature around the band gap can be seen in the band structures for −H and −OH terminated ribbons (Figure 1b). It can be understood because the dispersed states around the gap converge toward similar energies at *X*, necessarily imposing more rapid dispersion when the band gap at Γ is smaller.

An alternative route to control the ribbon band gap is through asymmetric functionalization of the two ribbon edges. Different configurations of graphene edge hydrogenation (−H) have been studied in the literature, and doubly hydrogenated (−2H) armchair graphene edges have been identified as the most stable.[22,31,32] The three possible cases with constant

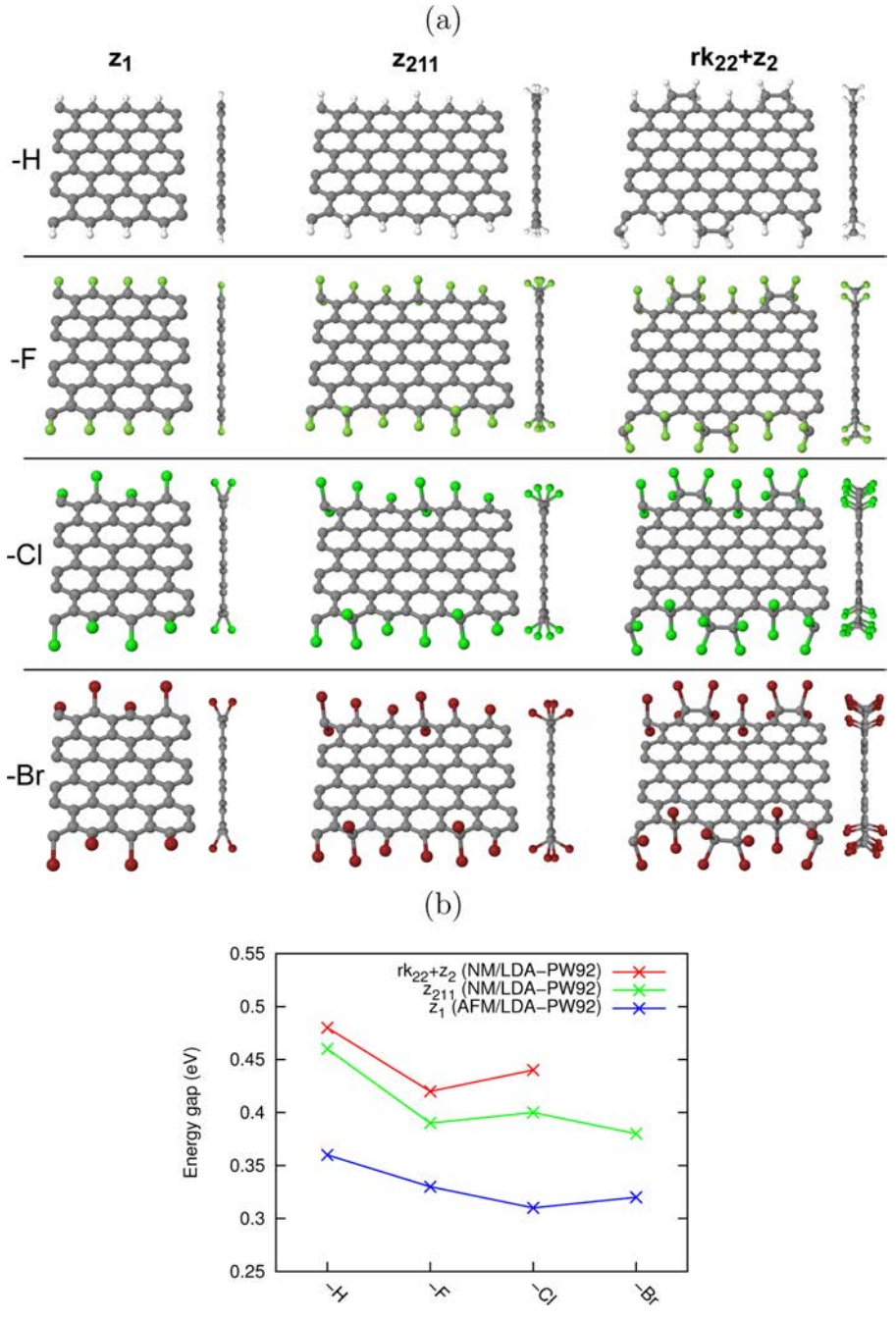

Figure 3. (a) Perspective and side view of the edge configurations z_1, z_{211}, and $rk_{22} + z_2$ (from left to right column) with different edge-functional groups −H, −F, −Cl, and −Br (from top to bottom) for width 6 GNRs. Edge formation energies are given in Table 1. (b) Calculated band gaps (LDA-PW92) for the different functionalized zigzag and reconstructed Klein GNRs. NM, nonmagnetic; AFM, antiferromagnetic.

hydrogen densities along each edge, "−H/−H", "−2H/−H", and "−2H/−2H", are shown in Figure 2a. The edge stability does not vary with ribbon width in the width range 6−15 (~6.05−17.05 Å); thus opposing armchair edges can be considered as energetically decoupled down to very small widths (<10 Å).[23]

The band gap for ribbons with these different edge terminations is shown in Figure 2b. The band gaps for the most widely studied case of a symmetric "−H/−H" edge hydrogenation are in good agreement with previous studies, reflecting a characteristic 3*N* periodicity.[7,18,54,55] For the other two opposed edge combinations, a shift is visible, demonstrating that doubly hydrogenating an armchair edge reduces the effective ribbon width by 1. This principle has also been observed in the literature,[32,56] and can be understood as a reduction of the sp^2 carbon network (see Figure 2a). Shifting the effective ribbon width in this way, that is, by modifying the edge-functionalization asymmetrically, results in significant band gap modification (for the width 7 AGNR, the gap varies over a 1.24 eV range; see Figure 2b).

This demonstrates a general principle, that asymmetry in functionalization (resulting in a change in hybridization of edge carbon atoms) between opposed edges of a graphene nanoribbon is another route to control the ribbon band gap. This could be achieved by attaching different functional groups

Table 1. Edge Formation Energy E_{edge}[22,32] and Calculated LDA-PW92 Band Gap for Different Functionalized Zigzag, Reconstructed Klein-type (Both Width 6), and Armchair (Width 7) Graphene Nanoribbons[a]

	zigzag		recon. Klein types			armchair	
LDA-PW92	z_1	z_{211}	$rk_{22} + z_2$	rk_{11}	rk_{22}	a_{11}	a_{22}
E_{edge} (eV/Å)							
−H	+0.100	−0.011	−0.107	+0.303	−0.047	+0.019	−0.174
−F	−0.580	−0.951	−1.512	−0.350	−1.436	−0.722	−1.690
−Cl	+0.140	+0.057	+0.136	+0.246	+0.563	+0.041	−0.006
−Br	+0.319	+0.325	+0.601	+0.411	unstable	+0.236	unstable
−S	+0.164		+0.753	+0.445	+0.584	+0.068	
−SH	+0.154			+0.233		−0.005	
−OH	−0.985			−0.723		−0.617	
band gap (eV)							
−H	0.36	0.46	0.48	0.00	0.33	1.59	0.35
−F	0.33	0.39	0.42	0.00	0.36	1.09	0.26
−Cl	0.31	0.40	0.44	0.00		1.07	0.31
−Br	0.32	0.38	0.14	0.00		1.09	
−S	0.00		0.42	0.00	0.30	0.90	
−SH	0.06			0.00		0.76	
−OH	0.16			0.00		0.76	

[a] *z*, zigzag; *rk*, reconstructed Klein; *a*, armchair; subscripts indicate number of functional atoms per edge carbon atom.[32]

to the two opposed ribbon edges,[39] or in other ways, for example by attaching ribbons orthogonally to a substrate.

A similar period three variation is reflected in the electron and hole effective masses, presented in Figure 2c. Varying the edge-functionalization for the width 7 ribbon shifts this periodicity as for the band gap, and can result in a near 7-fold decrease in the carrier effective masses, which is likely to have a significant effect on carrier mobility. Interestingly, some asymmetry is observed in the $(3n + 1)$ width ribbons, which have slightly lower hole than electron effective masses.

Zigzag Graphene Nanoribbons (ZGNRs). The structural behavior and influence on electronic properties of edge-functional groups attached to ZGNRs are next investigated for width 6 ZGNR (∼11.3 Å wide), as shown in Figure 3. As for AGNRs, in general the effect of interaction between neighboring functional groups needs to be taken into account. On the perfect zigzag edge, the carbon−carbon distance is ∼2.46 Å. Because this is more than twice the hydrogen van der Waals radius (1.10 Å[57]), it suggests that steric hindrance at hydrogenated zigzag edges should be negligible. However, for species such as Cl and Br with van der Waals radii of 1.75 and 1.83 Å, respectively,[58] significant interactions are expected. Steric hindrance between F atoms (van der Waals radius of 1.47 Å) attached to zigzag edges is expected to be weaker, and to compete against the preference for fully conjugated planar sp^2 carbon network geometry of the nanoribbon.

These steric out-of-plane effects are visible in Figure 3a, where both chlorinated and brominated z_1 edges exhibit rippling, with significant out-of-plane displacement of the functional groups (0.84 Å for Cl, 0.97 Å for Br). The ripple periodicity is a systematic alternation of neighboring functional groups, maximizing the spacing between the edge-functional groups; longer period ripples are found to be less stable.

The most stable edge configuration for hydrogenated ZGNRs was previously shown to be the nonmagnetic z_{211} structure,[22,59] where every third edge carbon atom is doubly hydrogenated. Similarly, we find here that of the various edge configurations considered, the z_{211} is the most stable irrespective of functional group −H, −F, −Cl (see Table 1). The exception is bromination, where pairwise addition is unfavored. Additionally, the z_{211} configuration provides an alternative mechanism for strain relief because the functional groups on a doubly functionalized sp^3-carbon already lie out-of-plane. Hence, in the z_{211} configuration, out-of-plane rippling is much less prominent. In any case, the presence of the sp^3 coordinated edge species means that such ribbon edges will not remain flat on a substrate.

All of the z_1 edge configurations are most stable in the antiferromagnetic ground state (except −S, which is metallic), similarly to hydrogenated ribbons.[9,16,22] The hydrogenated, fluorinated, chlorinated, and brominated zigzag ribbons all exhibit significant band gaps, which further increase in the more stable, nonmagnetic, z_{211} configuration (see Figure 3b). We note that these are LDA band gaps, and as discussed above are about ∼20−30% underestimated as compared to calculations using HSE03. Nonetheless, these gaps are smaller than equivalent width armchair ribbons, and notably there is significantly less variation in band gap with functional group (less than 0.08 eV).

We also considered functionalization of the related 5−7 zigzag edge, formed by rotating alternate carbon bonds along the ribbon edge,[23,60] but found in test calculations always to be less stable than the functionalized zigzag edges presented above.

Reconstructed Klein Graphene Nanoribbons (RKGNRs). When cutting a graphene sheet along the $\langle 2\bar{1}\bar{1}0 \rangle$ direction, two parallel cutting lines are possible, resulting in either zigzag or Klein edges. As reported previously, the most stable hydrogenated edge structures along this direction are not zigzag edges, but reconstructed variants of the Klein edge.[32] Thus, we have also considered similar functionalized reconstructed Klein ribbon edges (see Figure 3 and Table 1). The effective ribbon width definition is taken from ref 32, and hence reconstructed Klein-based GNRs have more carbon atoms per unit cell than zigzag GNRs, because the reconstructed Klein sp^3-carbon atoms are not included when determining the width. The similarity in calculated band gaps for the z_{211} and $rk_{22} + z_2$ terminated ribbons further supports this definition of effective ribbon width.

As can be seen in Table 1, fluorinated reconstructed Klein ribbons demonstrate the same trend in energetic stability as

hydrogenated ribbons. In both cases, the most stable edge configuration is the $rk_{22} + z_2$, where all edge carbon atoms are fully sp^3 coordinated. However, for the chlorinated and brominated ribbons, the reconstructed Klein-based ribbons are less stable than their zigzag analogues due to the significant steric hindrance between the functional groups.

Consistency in calculated band gaps has been found between the most stable functionalized zigzag and reconstructed Klein graphene nanoribbons, which are relatively insensitive to the choice of edge-functional group.

CONCLUSION

In summary, we have studied different edge-functionalized graphene nanoribbon types, armchair, zigzag, and reconstructed Klein GNRs. All edge-functional groups except hydrogen tested on armchair GNRs (−F, −Cl, −Br, −S, −OH, −SH) lead to characteristic edge rippling. Similar behavior has also been found for the bulkier −Cl and −Br edge-functional groups, when attached to zigzag z_1 GNRs, while for −H and −F the z_1 zigzag structures stay flat in-plane. However, for −H, −F, and −Cl functionalized zigzag ribbons, the nonmagnetic z_{211} configuration is more energetically stable than the z_1, and edge rippling is reduced. An even more stable ribbon configuration was found for −H and −Cl edge-functionalization, through changing the zigzag graphene edge structure to form a regular mix of zigzag and reconstructed Klein edges, called $rk_{22} + z_2$ GNRs. For these edge structures, steric hindrance is less prominent, and thus rippling is expected to occur rarely.

Regarding electronic properties, in particular the ribbon band gap, two general conclusions can be drawn. First, for thin armchair GNRs, the band gap can be tuned over a wide range $\Delta E_{gap} \approx 1.2$ eV, while for thin zigzag and reconstructed Klein GNR types, the band gap is largely insensitive to edge-functionalization. Second, the difference in band gap between z_1 and z_{211} zigzag GNRs and the new $rk_{22} + z_2$ reconstructed Klein GNR is small (considering similar ribbon widths, not including sp^3 hybridized reconstructed Klein carbons), and all of the most stable structures exhibit nonmagnetic ground states. Carrier effective mass in AGNRs are also highly dependent on ribbon width and edge-functionalization, with smaller gaps imposing more rapid band dispersion and hence lower effective masses. These results clearly favor thin armchair GNRs as possible candidates to design electronic properties via control of edge-functionalization.

AUTHOR INFORMATION

Corresponding Author

*E-mail: chris.ewels@cnrs-imn.fr.

Notes

The authors declare no competing financial interest.

ACKNOWLEDGMENTS

P.W., C.P.E., L.M., P.P., S.R., and V.V.I. thank the NANOSIM-GRAPHENE project no. ANR-09-NANO-016-01 funded by the French National Research Agency (ANR) in the frame of its 2009 programme in Nanosciences, Nanotechnologies & Nanosystems (P3N2009). P.W., C.P.E., J.-J.A., and B.H. thank the SPRINT project ANR-10-BLAN-0819. S.R. acknowledges funding support from the Spanish Ministry of Economy and Competitiveness (MAT2012-33911). We thank the CCIPL, CLUSTUS (IMN), and GENCI (Grant 2013-097015) for computing time. We thank COST project MP0901 NanoTP for support.

REFERENCES

(1) Geim, A. K.; Novoselov, K. S. The rise of graphene. *Nat. Mater.* **2007**, *6*, 183−191.

(2) Avouris, P.; Chen, Z.; Perebeinos, V. Carbon-based electronics. *Nat. Nanotechnol.* **2007**, *2*, 605−615.

(3) Novoselov, K. S.; Fal'ko, V. I.; Colombo, L.; Gellert, P. R.; Schwab, M. G.; Kim, K. A roadmap for graphene. *Nature* **2012**, *490*, 192−200.

(4) Neto, A. H. C.; Novoselov, K. New directions in science and technology: two-dimensional crystals. *Rep. Prog. Phys.* **2011**, *74*, 082501.

(5) Nakada, K.; Fujita, M.; Dresselhaus, G.; Dresselhaus, M. S. Edge state in graphene ribbons: Nanometer size effect and edge shape dependence. *Phys. Rev. B* **1996**, *54*, 17954−17961.

(6) Son, Y.-W.; Cohen, M. L.; Louie, S. G. Energy Gaps in Graphene Nanoribbons. *Phys. Rev. Lett.* **2006**, *97*, 216803.

(7) Barone, V.; Hod, O.; Scuseria, G. E. Electronic Structure and Stability of Semiconducting Graphene Nanoribbons. *Nano Lett.* **2006**, *6*, 2748−2754.

(8) Yang, L.; Park, C.-H.; Son, Y.-W.; Cohen, M. L.; Louie, S. G. Quasiparticle Energies and Band Gaps in Graphene Nanoribbons. *Phys. Rev. Lett.* **2007**, *99*, 186801.

(9) Son, Y.-W.; Cohen, M. L.; Louie, S. G. Half-metallic graphene nanoribbons. *Nature* **2006**, *444*, 347−349.

(10) Ritter, K. A.; Lyding, J. W. The influence of edge structure on the electronic properties of graphene quantum dots and nanoribbons. *Nat. Mater.* **2009**, *8*, 235−242.

(11) Terrones, M.; Botello-Méndez, A. R.; Campos-Delgado, J.; López-Urías, F.; Vega-Cantú, Y. I.; Rodríguez-Macías, F. J.; Elías, A. L.; Munoz-Sandoval, E.; Cano-Márquez, A. G.; Charlier, J.-C.; Terrones, H. Graphene and graphite nanoribbons: Morphology, properties, synthesis, defects and applications. *Nano Today* **2010**, *5*, 351−372.

(12) Acik, M.; Chabal, Y. J. Nature of Graphene Edges: A Review. *Jpn. J. Appl. Phys.* **2011**, *50*, 070101.

(13) Wakabayashi, K.; Dutta, S. Nanoscale and edge effect on electronic properties of graphene. *Solid State Commun.* **2012**, *152*, 1420−1430.

(14) Hod, O.; Barone, V.; Peralta, J. E.; Scuseria, G. E. Enhanced Half-Metallicity in Edge-Oxidized Zigzag Graphene Nanoribbons. *Nano Lett.* **2007**, *7*, 2295−2299.

(15) Cervantes-Sodi, F.; Csányi, G.; Piscanec, S.; Ferrari, A. C. Edge-functionalized and substitutionally doped graphene nanoribbons: Electronic and spin properties. *Phys. Rev. B* **2008**, *77*, 165427.

(16) Lee, G.; Cho, K. Electronic structures of zigzag graphene nanoribbons with edge hydrogenation and oxidation. *Phys. Rev. B* **2009**, *79*, 165440.

(17) Lu, Y. H.; Wu, R. Q.; Shen, L.; Yang, M.; Sha, Z. D.; Cai, Y. Q.; He, P. M.; Feng, Y. P. Effects of edge passivation by hydrogen on electronic structure of armchair graphene nanoribbon and band gap engineering. *Appl. Phys. Lett.* **2009**, *94*, 122111−122113.

(18) Wagner, P.; Ewels, C. P.; Ivanovskaya, V. V.; Briddon, P. R.; Pateau, A.; Humbert, B. Ripple edge engineering of graphene nanoribbons. *Phys. Rev. B* **2011**, *84*, 134110.

(19) Wu, X.-j.; Wu, M.-h.; Zeng, X. C. Chemically decorated boron-nitride nanoribbons. *Front. Phys. China* **2009**, *4*, 367−372.

(20) Lopez-Bezanilla, A.; Huang, J.; Terrones, H.; Sumpter, B. G. Boron Nitride Nanoribbons Become Metallic. *Nano Lett.* **2011**, *11*, 3267−3273.

(21) Lopez-Bezanilla, A.; Huang, J.; Terrones, H.; Sumpter, B. G. Structure and Electronic Properties of Edge-Functionalized Armchair Boron Nitride Nanoribbons. *J. Phys. Chem. C* **2012**, *116*, 15675−15681.

(22) Wassmann, T.; Seitsonen, A. P.; Saitta, A. M.; Lazzeri, M.; Mauri, F. Structure, Stability, Edge States, and Aromaticity of Graphene Ribbons. *Phys. Rev. Lett.* **2008**, *101*, 096402.

(23) Koskinen, P.; Malola, S.; Häkkinen, H. Self-Passivating Edge Reconstructions of Graphene. *Phys. Rev. Lett.* **2008**, *101*, 115502.
(24) Zobelli, A.; Ivanovskaya, V.; Wagner, P.; Suarez-Martinez, I.; Yaya, A.; Ewels, C. P. A comparative study of density functional and density functional tight binding calculations of defects in graphene. *Phys. Status Solidi B* **2012**, *249*, 276−282.
(25) Wakabayashi, K.; Fujita, M.; Ajiki, H.; Sigrist, M. Electronic and magnetic properties of nanographite ribbons. *Phys. Rev. B* **1999**, *59*, 8271−8282.
(26) Branicio, P. S.; Jhon, M. H.; Gan, C. K.; Srolovitz, D. J. Properties on the edge: graphene edge energies, edge stresses, edge warping, and the Wulff shape of graphene flakes. *Modell. Simul. Mater. Sci. Eng.* **2011**, *19*, 054002.
(27) Liu, Z.; Suenaga, K.; Harris, P. J. F.; Iijima, S. Open and Closed Edges of Graphene Layers. *Phys. Rev. Lett.* **2009**, *102*, 015501.
(28) Xie, L.; Wang, H.; Jin, C.; Wang, X.; Jiao, L.; Suenaga, K.; Dai, H. Graphene Nanoribbons from Unzipped Carbon Nanotubes: Atomic Structures, Raman Spectroscopy, and Electrical Properties. *J. Am. Chem. Soc.* **2011**, *133*, 10394−10397.
(29) Suenaga, K.; Koshino, M. Atom-by-atom spectroscopy at graphene edge. *Nature* **2010**, *468*, 1088.
(30) Klein, D. Graphitic polymer strips with edge states. *Chem. Phys. Lett.* **1994**, *217*, 261.
(31) Ivanovskaya, V. V.; Zobelli, A.; Wagner, P.; Heggie, M. I.; Briddon, P. R.; Rayson, M. J.; Ewels, C. P. Low-Energy Termination of Graphene Edges via the Formation of Narrow Nanotubes. *Phys. Rev. Lett.* **2011**, *107*, 065502.
(32) Wagner, P.; Ivanovskaya, V. V.; Melle-Franco, M.; Humbert, B.; Adjizian, J.-J.; Briddon, P. R.; Ewels, C. P. Stable hydrogenated graphene edge types: Normal and reconstructed Klein edges. *Phys. Rev. B* **2013**, *88*, 094106.
(33) Cai, J.; Ruffieux, P.; Jaafar, R.; Bieri, M.; Braun, T.; Blankenburg, S.; Muoth, M.; Seitsonen, A. P.; Saleh, M.; Feng, X.; Mullen, K.; Fasel, R. Atomically precise bottom-up fabrication of graphene nanoribbons. *Nature* **2010**, *466*, 470−473.
(34) Dubois, S. M.-M.; Lopez-Bezanilla, A.; Cresti, A.; Triozon, F.; Biel, B.; Charlier, J.-C.; Roche, S. Quantum Transport in Graphene Nanoribbons: Effects of Edge Reconstruction and Chemical Reactivity. *ACS Nano* **2010**, *4*, 1971−1976.
(35) Cocchi, C.; Ruini, A.; Prezzi, D.; Caldas, M. J.; Molinari, E. Designing All-Graphene Nanojunctions by Covalent Functionalization. *J. Phys. Chem. C* **2011**, *115*, 2969−2973.
(36) Selli, D.; Baldoni, M.; Sgamellotti, A.; Mercuri, F. Redox-switchable devices based on functionalized graphene nanoribbons. *Nanoscale* **2012**, *4*, 1350−1354.
(37) Rosenkranz, N.; Till, C.; Thomsen, C.; Maultzsch, J. Ab initio calculations of edge-functionalized armchair graphene nanoribbons: Structural, electronic, and vibrational effects. *Phys. Rev. B* **2011**, *84*, 195438.
(38) Jippo, H.; Ohfuchi, M. First-principles study of edge-modified armchair graphene nanoribbons. *J. Appl. Phys.* **2013**, *113*, 183715−183715−6.
(39) Martin-Martinez, F. J.; Fias, S.; Lier, G. V.; Proft, F. D.; Geerlings, P. Tuning aromaticity patterns and electronic properties of armchair graphene nanoribbons with chemical edge functionalisation. *Phys. Chem. Chem. Phys.* **2013**, DOI: 10.1039/C3CP51293B.
(40) Perdew, J. P.; Wang, Y. Accurate and simple analytic representation of the electron-gas correlation energy. *Phys. Rev. B* **1992**, *45*, 13244−13249.
(41) Perdew, J. P.; Burke, K.; Ernzerhof, M. Generalized Gradient Approximation Made Simple. *Phys. Rev. Lett.* **1996**, *77*, 3865−3868.
(42) Briddon, P. R.; Jones, R. LDA Calculations Using a Basis of Gaussian Orbitals. *Phys. Status Solidi B* **2000**, *217*, 131−171.
(43) Rayson, M. J.; Briddon, P. R. Highly efficient method for Kohn-Sham density functional calculations of 500−10000 atom systems. *Phys. Rev. B* **2009**, *80*, 205104.
(44) Briddon, P. R.; Rayson, M. J. Accurate Kohn-Sham DFT with the speed of tight binding: Current techniques and future directions in materials modelling. *Phys. Status Solidi B* **2011**, *248*, 1309−1318.
(45) Hartwigsen, C.; Goedecker, S.; Hutter, J. Relativistic separable dual-space Gaussian pseudopotentials from H to Rn. *Phys. Rev. B* **1998**, *58*, 3641.
(46) Kresse, G.; Hafner, J. Ab initio molecular dynamics for liquid metals. *Phys. Rev. B* **1993**, *47*, 558−561.
(47) Heyd, J.; Scuseria, G. E.; Ernzerhof, M. Hybrid functionals based on a screened Coulomb potential. *J. Chem. Phys.* **2003**, *118*, 8207−8215.
(48) Jain, M.; Chelikowsky, J. R.; Louie, S. G. Reliability of Hybrid Functionals in Predicting Band Gaps. *Phys. Rev. Lett.* **2011**, *107*, 216806.
(49) Ferretti, A.; Mallia, G.; Martin-Samos, L.; Bussi, G.; Ruini, A.; Montanari, B.; Harrison, N. M. Ab initio complex band structure of conjugated polymers: Effects of hydrid density functional theory and GW schemes. *Phys. Rev. B* **2012**, *85*, 235105.
(50) Prezzi, D.; Varsano, D.; Ruini, A.; Marini, A.; Molinari, E. Optical properties of graphene nanoribbons: The role of many-body effects. *Phys. Rev. B* **2008**, *77*, 041404.
(51) Ruffieux, P.; Cai, J.; Plumb, N. C.; Patthey, L.; Prezzi, D.; Ferretti, A.; Molinari, E.; Feng, X.; Müllen, K.; Pignedoli, C. A.; Fasel, R. Electronic Structure of Atomically Precise Graphene Nanoribbons. *ACS Nano* **2012**, *6*, 6930−6935.
(52) Long, M.-Q.; Tang, L.; Wang, D.; Wang, L.; Shuai, Z. Theoretical Predictions of Size-Dependent Carrier Mobility and Polarity in Graphene. *J. Am. Chem. Soc.* **2009**, *131*, 17728−17729.
(53) Wang, J.; Zhao, R.; Yang, M.; Liu, Z.; Liu, Z. Inverse relationship between carrier mobility and bandgap in graphene. *J. Chem. Phys.* **2013**, *138*, 084701−084701−5.
(54) Baldoni, M.; Sgamellotti, A.; Mercuri, F. Electronic properties and stability of graphene nanoribbons: An interpretation based on Clar sextet theory. *Chem. Phys. Lett.* **2008**, *464*, 202−207.
(55) Wassmann, T.; Seitsonen, A. P.; Saitta, A. M.; Lazzeri, M.; Mauri, F. Clars Theory, π -Electron Distribution, and Geometry of Graphene Nanoribbons. *J. Am. Chem. Soc.* **2010**, *132*, 3440−3451.
(56) Zheng, X. H.; Huang, L. F.; Wang, X. L.; Lan, J.; Zeng, Z. Band gap engineering in armchair-edged graphene nanoribbons by edge dihydrogenation. *Comput. Mater. Sci.* **2012**, *62*, 93−98.
(57) Rowland, R. S.; Taylor, R. Intermolecular Nonbonded Contact Distances in Organic Crystal Structures: Comparison with Distances Expected from van der Waals Radii. *J. Phys. Chem.* **1996**, *100*, 7384−7391.
(58) Mantina, M.; Chamberlin, A. C.; Valero, R.; Cramer, C. J.; Truhlar, D. G. Consistent van der Waals Radii for the Whole Main Group. *J. Phys. Chem. A* **2009**, *113*, 5806−5812.
(59) Kunstmann, J.; Ozdoğan, C.; Quandt, A.; Fehske, H. Stability of edge states and edge magnetism in graphene nanoribbons. *Phys. Rev. B* **2011**, *83*, 045414.
(60) Koskinen, P.; Malola, S.; Häkkinen, H. Evidence for graphene edges beyond zigzag and armchair. *Phys. Rev. B* **2009**, *80*, 73401.